

# Fluorescent Derivatives of $\sigma$ Receptor Ligand 1-Cyclohexyl-4-[3-(5-methoxy-1,2,3,4-tetrahydronaphthalen-1-yl)propyl]piperazine (PB28) as a Tool for Uptake and Cellular Localization Studies in Pancreatic Tumor Cells

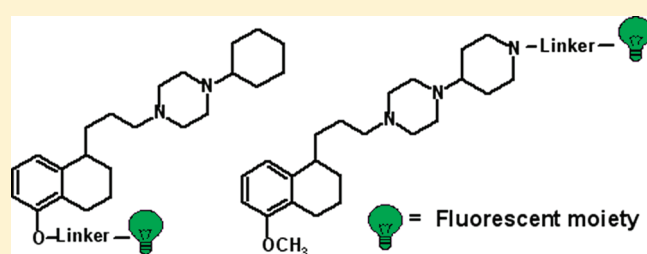
Carmen Abate,<sup>\*,†</sup> John R. Hornick,<sup>‡</sup> Dirk Spitzer,<sup>‡</sup> William G. Hawkins,<sup>‡</sup> Mauro Niso,<sup>†</sup> Roberto Perrone,<sup>†</sup> and Francesco Berardi<sup>†</sup>

<sup>†</sup>Dipartimento Farmacochimico, Università degli Studi di Bari "Aldo Moro", Via Orabona 4, I-70125 Bari, Italy

<sup>‡</sup>Division of Hepatobiliary, Pancreatic, and Gastrointestinal Surgery, Department of Surgery, Washington University School of Medicine, St. Louis, Missouri, United States

**S** Supporting Information

**ABSTRACT:** Fluorescent derivatives of  $\sigma_2$  high affinity ligand 1-cyclohexyl-4-[3-(5-methoxy-1,2,3,4-tetrahydronaphthalen-1-yl)propyl]piperazine **1** (PB28) were synthesized. NBD or dansyl fluorescent tags were connected through a 5- or 6-atom linker in two diverse positions of **1** structure. Good  $\sigma_2$  affinities were obtained when the fluorescent tag was linked to 5-methoxytetralin nucleus replacing the methyl function. NBD-bearing compound **16** displayed high  $\sigma_2$  affinity ( $K_i = 10.8$  nM) and optimal fluorescent properties. Its uptake in pancreatic tumor cells was evaluated by flow cytometry, showing that it partially occurs through endocytosis. In proliferating cells, the uptake was higher supporting that  $\sigma_2$  receptors are markers of cell proliferation and that the higher the proliferation is, the stronger the antiproliferative effect of  $\sigma_2$  agonists is. Colocalization of **16** with subcellular organelles was studied by confocal microscopy: the greatest was in endoplasmic reticulum and lysosomes. Fluorescent  $\sigma_2$  ligands show their potential in clarifying the mechanisms of action of  $\sigma_2$  receptors.



## INTRODUCTION

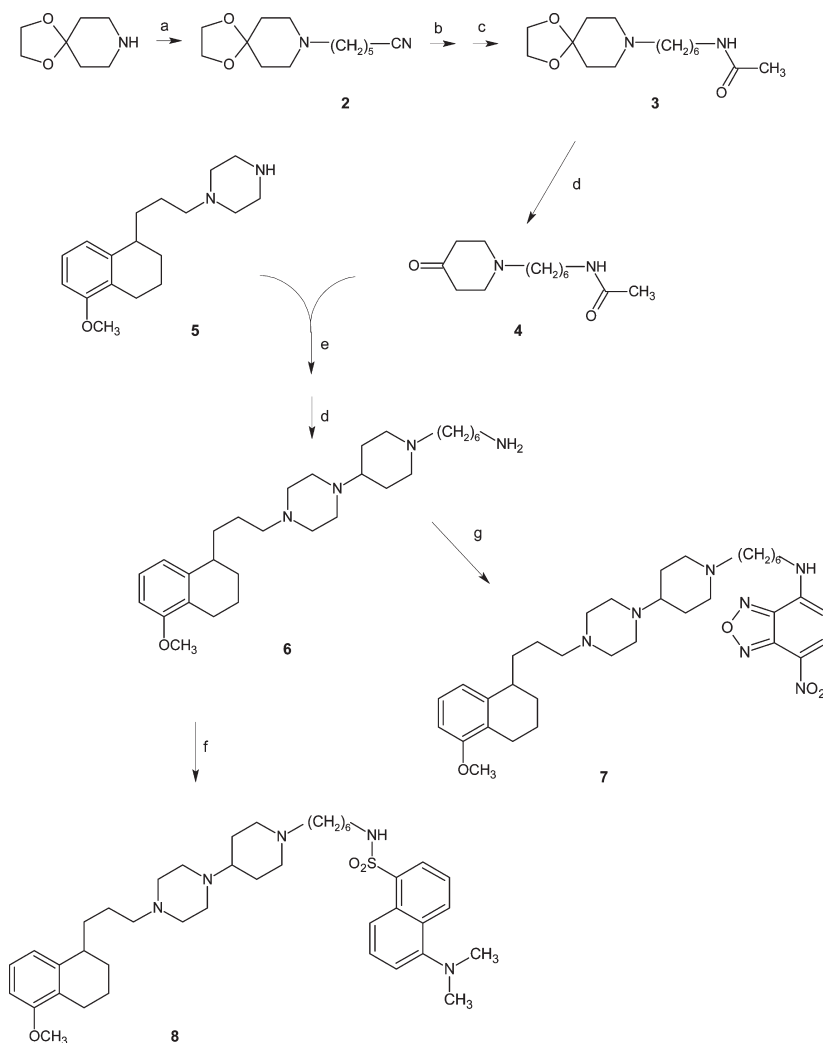
After their first discovery in 1976, sigma ( $\sigma$ ) receptor research met a renovated enthusiasm in the early 1990s when the two subtypes,  $\sigma_1$  and  $\sigma_2$ , were identified.<sup>1</sup> The  $\sigma_1$  subtype was soon thereafter isolated and cloned from different sources,<sup>2</sup> and it has been recently classified as a receptor chaperone at the endoplasmic reticulum (ER) membrane that regulates ER-mitochondrial  $\text{Ca}^{2+}$  signaling and cell survival.<sup>3</sup> Although their mechanism of action is still unclear,  $\sigma$  proteins receive much interest because of their potential applications as drug targets for a wide range of diseases.  $\sigma_1$  receptor ligands display neuroprotective and neuroregulative functions and are under evaluation for the treatment of a number of neurological disorders<sup>4</sup> such as depression,<sup>5</sup> schizophrenia,<sup>6</sup> Alzheimer's and Parkinson's diseases,<sup>7–9</sup> and for drug abuse (e.g., cocaine).<sup>10</sup> The high therapeutic potential of  $\sigma_2$  receptors comes from the evidence that this subtype is overexpressed in a wide variety of cancer tissues, and activation of  $\sigma_2$  receptors lead tumor cells to death through different apoptotic pathways.<sup>11–13</sup> Therefore, a number of  $\sigma_2$  receptor ligands are under investigation for cancer treatment and diagnosis.<sup>14–16</sup> Nevertheless, the  $\sigma_2$  subtype is not as well characterized as the  $\sigma_1$ . It has not yet been cloned, and attempted characterization from homogenate of  $\sigma_2$ -overexpressing tumor cells led to isolation of histone proteins by affinity chromatography.<sup>17</sup> The  $\sigma_2$

selector used was a derivative of 1-cyclohexyl-4-[3-(5-methoxy-1,2,3,4-tetrahydronaphthalen-1-yl)-*n*-propyl]piperazine (**1**, PB28), one of the highest affinity  $\sigma_2$  receptor ligands known,<sup>18,19</sup> concluding that either  $\sigma_2$  receptors may be histones or histone binding proteins or compound **1** binds such proteins as well as  $\sigma_2$  receptors, with modeling studies conducted to rationalize these hypotheses.<sup>20</sup> Such results were in disagreement with findings from fluorescence microscopy, which localizes  $\sigma_2$  subtypes in several organelles except the nucleus through the use of fluorescent  $\sigma_2$  ligands.<sup>21,22</sup> Besides the intracellular localization, there are other ambiguities related to the  $\sigma_2$  receptors: evidence shows that  $\sigma_2$  ligands activate different apoptotic pathways in diverse tumor cells.<sup>11–13,23</sup> With the aim of helping to clarify some of these ambiguities, we synthesized a small series of fluorescent derivatives of compound **1** to be used in microscopy studies for the purpose of localizing  $\sigma_2$  receptors subcellularly within cancer cells.

Intrinsically fluorescent compound **1** analogues have been synthesized in the past, with appreciable  $\sigma$  receptor affinity but with maximum excitation and emission wavelength ( $\lambda_{\text{exc}}$  and  $\lambda_{\text{em}}$ ) inappropriate for use in living cells for fluorescence

Received: May 11, 2011

Published: July 11, 2011

Scheme 1. Synthesis of Fluorescent Compound 1 Analogues: Fluorescent Tag at the Piperazine<sup>a</sup>

<sup>a</sup> Reagents: (a) 6-Br(CH<sub>2</sub>)<sub>5</sub>CN; (b) LiAlH<sub>4</sub>; (c) CH<sub>3</sub>COCl; (d) HCl; (e) ZnCl<sub>2</sub>, NaCNBH<sub>3</sub>; (f) dansyl chloride; (g) NBD-chloride.

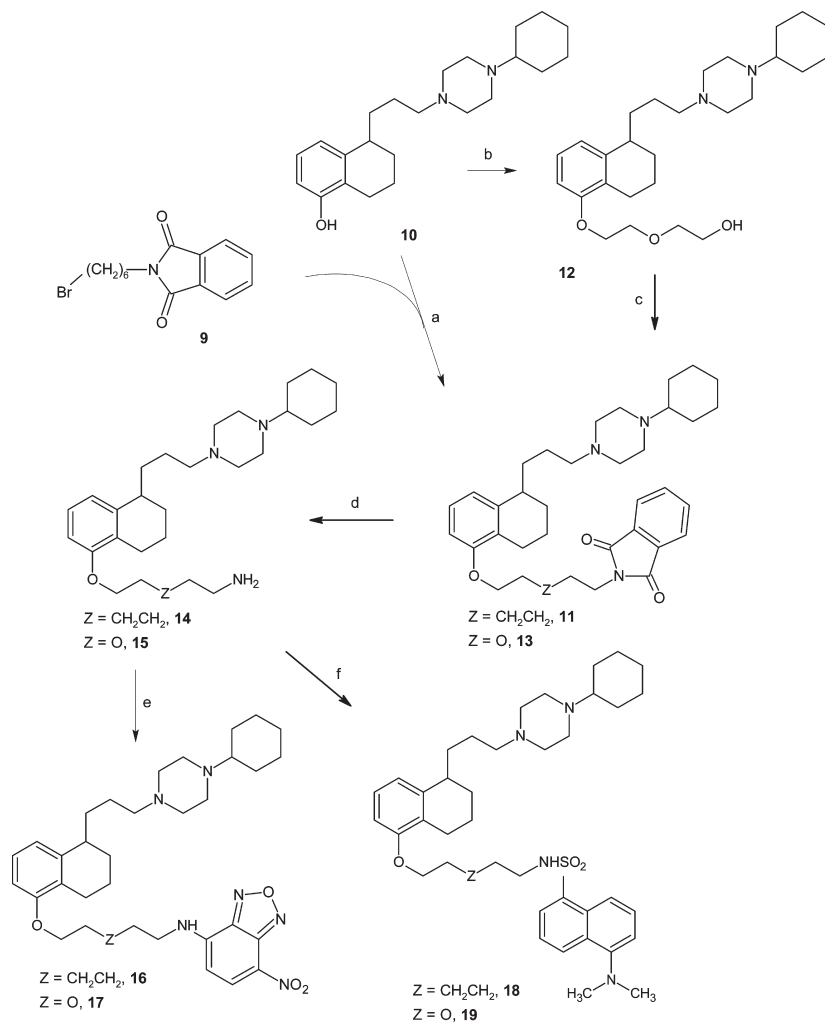
microscopy.<sup>24</sup> Therefore, we followed a common approach to overcome this limitation: dansyl ( $\lambda_{\text{exc}} \sim 315$  nm) and 7-nitro-2,1,3-benzoxadiazole (NBD) ( $\lambda_{\text{exc}} \sim 420$  nm) moieties were alternatively inserted in two different positions on compound 1 structure through a 5- or 6-atom linker. Such separation between the pharmacophore and the fluorescent tag should prevent the loss of affinity, leaving the fluorescent properties of the fluorescent moieties almost unchanged. Compound 16, with the best fluorescence/pharmacological properties, was used for preliminary fluorescence microscopy analyses in murine and human pancreatic tumor cells which have been previously shown to overexpress  $\sigma_2$  receptors.<sup>11</sup> Human pancreatic tumor cells (BxPC3) were selected for more extensive studies of compound 16, whose internalization and colocalization by confocal microscopy with subcellular organelles were evaluated.

## RESULTS AND DISCUSSION

**Chemistry.** The synthetic pathways for final compounds 7, 8, and 16–19 are depicted in Schemes 1 and 2. Key intermediate 6 was prepared starting from commercial piperidin-4-one ethylene ketal (1,4-dioxo-8-aza-spiro[4.5]decane), which was alkylated

with 6-bromohexanenitrile, affording intermediate 2. Upon reduction with LiAlH<sub>4</sub> to the corresponding amine and subsequent amine protection through acetylation, compound 2 provided derivative 3. Acidic deprotection of the ethylene–acetal function with HCl led to intermediate 4, which underwent reductive amination with piperazine 5,<sup>25</sup> providing the acetyl derivative of 6, which was deacetylated, affording key amine 6. Reaction of this latter alternatively with NBD-chloride or dansyl chloride afforded the fluorescent compounds 7 and 8, respectively (Scheme 1).

The final compounds 16–19 were synthesized as outlined in Scheme 2. The reaction between potassium phthalimide and 1,6-dibromohexane gave intermediate 9,<sup>26</sup> which was used to alkylate the key phenolic intermediate 10,<sup>19</sup> affording phthalimide 11. Alkylation of the phenolic intermediate 9 with 2-(2-chloroethoxy)-ethanol afforded the corresponding alcohol 12 that underwent Mitsunobu condensation with phthalimide in the presence of triphenylphosphine and diisopropylazodicarboxylate (DIAD) to yield compound 13. Phthalimide derivatives 11 and 13 underwent hydrazinolysis to afford intermediate primary amines 14 and 15, respectively. Reaction of 14 with NBD-chloride or dansyl chloride afforded the fluorescent compounds 16 and 18,

Scheme 2. Synthesis of Fluorescent Compound 1 Analogues: Fluorescent Tag at the Tetralin Nucleus<sup>a</sup>

<sup>a</sup> Reagents: (a)  $\text{K}_2\text{CO}_3$ ; (b)  $\text{ClCH}_2\text{CH}_2\text{OCH}_2\text{CH}_2\text{OH}$ ,  $\text{K}_2\text{CO}_3$ ; (c)  $\text{Ph}_3\text{P}$ , phthalimide, DIAD; (d) hydrazine hydrate; (e) NBD-chloride; (f) dansyl chloride.

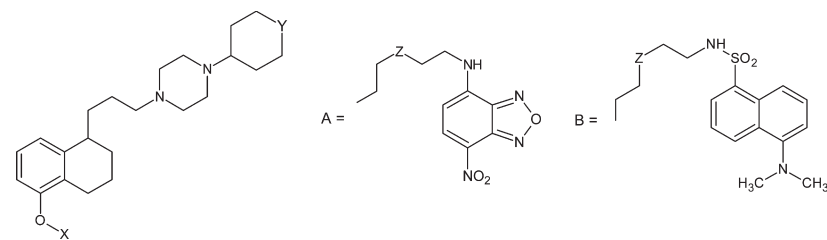
respectively. Reaction of 15 with NBD-chloride or dansyl chloride afforded respectively the fluorescent final compounds 17 and 19. All the final compounds were converted to the corresponding hydrochloride salts with gaseous HCl.

**Radioligand Binding and  $\sigma_1$  and  $\sigma_2$  Receptor Affinities.** Results from binding assays are expressed as inhibition constants ( $K_i$  values) in Table 1. The introduction of the fluorescent tag and the linker produced a decrease in the affinity at both  $\sigma$  receptors with respect to lead compound 1. The most dramatic drop in the affinity at both  $\sigma$  receptors was observed with compounds 7 ( $K_i = 2570$  nM for  $\sigma_1$  and  $K_i = 1720$  nM for  $\sigma_2$  receptor) and 8 ( $K_i > 5000$  nM for  $\sigma_1$  and  $K_i = 5020$  nM for  $\sigma_2$  receptor), which reached micromolar values. In such compounds, the piperidine ring replacing the cyclohexyl ring was functionalized with the fluorescent tag through a six-methylene chain. The drop in the affinity was independent from the nature of the fluorescent tag, indicating that functionalization (at least with a six-atom linker) in that position of the pharmacophore was not tolerated by the  $\sigma_2$  receptors, in accordance with a previous study in which substitution of the cyclohexyl with more hindered substituents led to reduced  $\sigma$  affinities.<sup>18,27</sup> On the other hand, fluorescent final compounds obtained through insertion of the

alkyl fluorescent tag on the 5-methoxy-tetralin ring in place of the methyl group displayed nanomolar affinities at both  $\sigma$  receptors (compounds 16–19). Previous SAfIR studies demonstrated how the methoxy substituent was unessential for  $\sigma_2$  receptor binding indeed.<sup>28</sup> NBD or dansyl moieties were tolerated at the  $\sigma_2$  receptor, with the highest affinity displayed by the NBD-bearing compound 16 ( $K_i = 10.8$  nM). The presence of the NBD, but not of the dansyl moiety, appeared to be detrimental ( $K_i = 78.8$  nM for 16 and  $K_i = 96.2$  nM for 17) for  $\sigma_1$  receptor binding. With  $\sigma_1$  and  $\sigma_2$  affinities in the same range, dansyl-bearing ligands 18 and 19 did not show any  $\sigma_2$  versus  $\sigma_1$  selectivity, whereas compounds bearing NBD (16 and 17) displayed a moderate  $\sigma_2$  selectivity (8-fold and 2.5-fold, respectively). Selectivity was missing in lead compound 1 when binding assays were performed on animal tissues according to literature protocols.<sup>18</sup> Results obtained with this small series of compounds demonstrated that a fluorescent tag spaced out from the tetralinoxy moiety by a 5- or 6-atom linker leads to molecules with good  $\sigma$  receptor affinities useful for in living cells visualization of  $\sigma_2$  receptors, with compound 16 displaying the best pharmacological properties for further investigation.

**Fluorescent Ligand Studies.** The fluorescent properties of final compounds are listed in Table 1. The excitation and emission

Table 1. Receptor Affinities and Fluorescence Properties of Final Compounds



compd	X	Y	Z	$K_1$ nM <sup>a</sup>		CHCl <sub>3</sub>			EtOH <sup>b</sup>			PBS <sup>b,c</sup>		$\epsilon^d$	
				$\sigma_1$	$\sigma_2$	$\lambda_{exc}$ (nm)	$\lambda_{em}$ (nm)	$\Phi$	$\lambda_{exc}$ (nm)	$\lambda_{em}$ (nm)	$\Phi$	$\lambda_{exc}$ (nm)	$\lambda_{em}$ (nm)		
1 <sup>e</sup>	CH <sub>3</sub>	CH <sub>2</sub>		0.38 ± 0.10	0.68 ± 0.20										
7	CH <sub>3</sub>	A	CH <sub>2</sub> CH <sub>2</sub>	2570 <sup>f</sup>	1720 ± 160	450	515	0.17	476	520	0.08	480	535	14391	
8	CH <sub>3</sub>	B	CH <sub>2</sub> CH <sub>2</sub>	>5000 <sup>f</sup>	5020 ± 180	346	490	0.32	335	507	0.29	340	510	2600	
16	A	CH <sub>2</sub>	CH <sub>2</sub> CH <sub>2</sub>	78.7 ± 18.2	10.8 ± 3.0	451	514	0.20	467	520	0.05	460	520	11300	
17	A	CH <sub>2</sub>	O	96.2 <sup>f</sup>	39.3 ± 11.8	450	512	0.18	465	520	0.04	460	520	6544	
18	B	CH <sub>2</sub>	CH <sub>2</sub> CH <sub>2</sub>	9.08 ± 1.32	20.8 ± 1.5	340	490	0.30	335	507	0.20	345	485	4000	
19	B	CH <sub>2</sub>	O	19.8 ± 8.7	25.7 ± 4.7	345	490	0.48	335	507	0.23	343	510	2741	
(+)-pentazocine				2.62 ± 0.25											
DTG					24.6 ± 2.2										

<sup>a</sup> Values are the means of  $n \geq 2$  separate experiments. <sup>b</sup> Fluorescence properties herein reported were evaluated on compounds as free bases, but they were also evaluated on their corresponding hydrochloride salts in EtOH and PBS solutions. A maximum of 5 nm shift was observed in the excitation and emission wavelengths when compared to the excitation and emission wavelengths from the corresponding free bases. <sup>c</sup> All compounds solubilized in PBS gave  $\Phi$  value very close to 0 and therefore they are not reported. <sup>d</sup> From EtOH solutions of compounds in EtOH. <sup>e</sup> From ref 18, where results from binding on human cells, in which compound 1 displays about 40-fold  $\sigma_2$  versus  $\sigma_1$  selectivity, are also reported. <sup>f</sup> From a unique experiment.

spectra were obtained from solution of the final compounds in organic solvents (EtOH and CHCl<sub>3</sub>) and in aqueous solution (PBS buffer). The NBD-bearing compounds (8, 16, 17) displayed excitation peaks at two different wavelengths (~335 and ~450 nm), and for both the wavelengths, the corresponding  $\lambda_{em}$  was ~520 nm. The  $\lambda_{exc}$  selected to perform the assays in living cells was 450 nm to avoid cells autofluorescence phenomena. Dansyl-bearing compounds (7, 18, 19) displayed a  $\lambda_{exc}$  more shifted toward the UV region (~340 nm). All of the compounds showed an important difference between  $\lambda_{exc}$  and  $\lambda_{em}$  (Stokes shift). Quantum yields ( $\Phi$ ) were determined in the above-mentioned solvents to probe the environment affecting the sensitivity of the final fluorescent ligands because the fluorophores selected (Dansyl and NBD) are endowed with environment sensitivity properties, (i.e., low quantum yield in aqueous solution but high fluorescence in nonpolar solvents or when bound to a hydrophobic sites). All tested compounds exhibited very low fluorescence in PBS buffer but became fluorescent in the organic solvents. The highest quantum yields were those recorded in CHCl<sub>3</sub> for all the final compounds:  $\Phi$  values were 2- or 4-fold higher in CHCl<sub>3</sub> than in EtOH for NBD-bearing compounds (8, 16, 17) and several-fold higher than in PBS buffer. Dansyl-bearing compounds (7, 18, 19) showed a less pronounced increase in  $\Phi$  values from EtOH to CHCl<sub>3</sub> solutions, although the highest  $\Phi$  was shown by compound 19 ( $\Phi = 0.48$ ). Molar extinction coefficients ( $\epsilon$ ) were determined for all final compounds (in EtOH), with the lowest values displayed by the dansyl-bearing compounds (2600–4000 L/mol·cm) and the highest values displayed by the NBD-bearing compounds (6544–14391 L/mol·cm), indicating that the fluorescence intensity of the latter compounds is stronger. Preliminary fluorescence microscopy experiments

were conducted with compound 16, which displayed the best combination between pharmacological ( $\sigma_2$  receptor affinity and selectivity) and fluorescence properties (convenient excitation and emission wavelengths and high  $\epsilon$  value), and promising results were obtained in different tumor pancreatic cells which were previously shown to overexpress  $\sigma_2$  receptors.<sup>11</sup> Therefore, compound 16 was evaluated in more details in in vitro internalization studies and cellular colocalization by confocal microscopy in human pancreatic tumor cells (BxPC3).

**In Vitro Internalization Studies.** Uptake of compound 16 in BxPC3 pancreatic cancer cells was analyzed immediately following treatment (25 nM) and the mean fluorescence recorded over time (Figure 1A). The  $T_{1/2}$  of maximum fluorescence at 60 min was  $7.8 \pm 1.5$  min (mean  $\pm$  SEM). We further studied uptake for the purpose of better understanding the involvement of endocytosis of these compounds and the receptor. Caveolin-mediated (lipid rafts-mediated) endocytosis can be inhibited by Filipin III<sup>29</sup> and clathrin-mediated endocytosis by phenylarsine oxide (PAO).<sup>30</sup> BxPC3 cells were pretreated with Filipin III (5  $\mu$ g/mL) or PAO (10 mM) for 30 min prior to treatment with compound 16 (25 nM) and mean fluorescence was collected over 60 min. The rate of uptake was decreased from  $7.8 \pm 1.5$  min to  $6.8 \pm 0.8$  min for Filipin III and  $4.9 \pm 2.1$  min for PAO. As well, the overall uptake at 60 min was decreased to 69% and 50% for Filipin III and PAO, respectively. Taken together, the  $T_{1/2}$  in the range of minutes, and the decreased uptake in the presence of endocytosis inhibitors suggest that the internalization of 16 occurs, in part, through the caveolin- and clathrin-mediated endocytotic pathways in addition to simple membrane diffusion. Uptake by the clathrin-dependent pathway has been described previously with other  $\sigma_2$  receptor ligands,<sup>21,22</sup> but uptake by the caveolin-

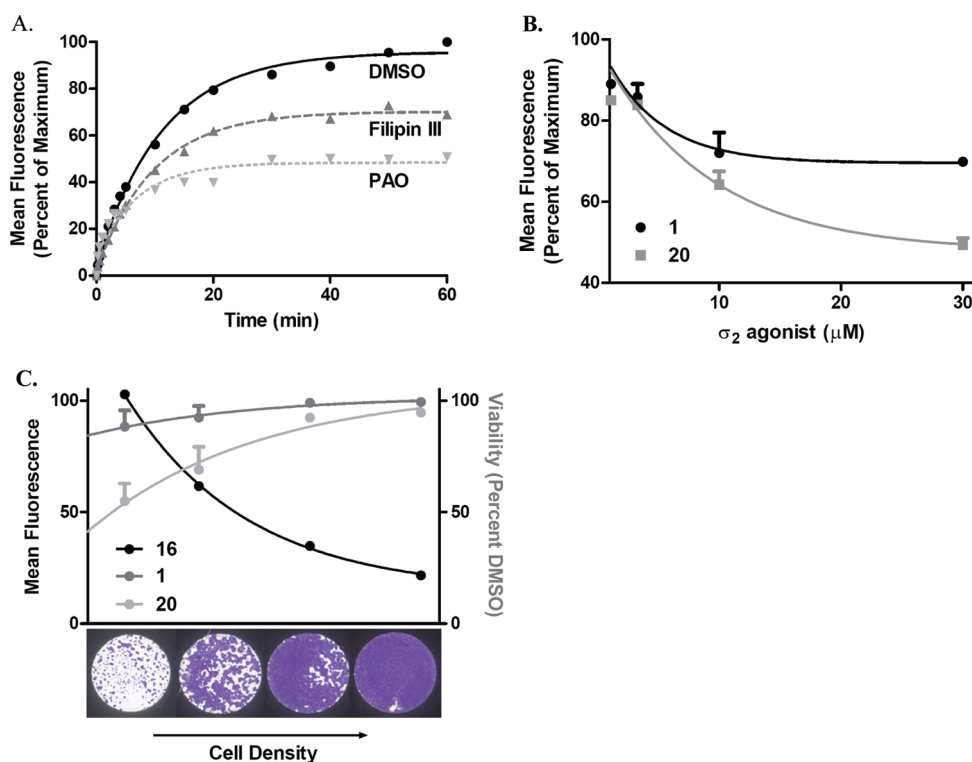


**Figure 1.** Cellular internalization of the fluorescent  $\sigma_2$  receptor ligand 16. (A) Kinetic uptake of compound 16: BxPC3 pancreatic cancer cells were treated for 1 h with the endocytosis inhibitors Filipin III ( $5 \mu\text{g}/\text{mL}$ ) or phenylarsine oxide (PAO,  $10 \mu\text{M}$ ) or DMSO vehicle for 60 min prior to kinetic uptake analysis of 16 ( $25 \text{ nM}$ ) by flow cytometry. Compound 16 uptake represents the percentage of the mean fluorescence of maximum signal intensity. (B) Competition of compound 16 by  $\sigma_2$  agonist structural analogues. BxPC3 cells were treated with increasing doses of compounds 1 or 20 for 45 min prior to replacement with compound 16 ( $25 \text{ nM}$ ) for 45 min and fluorescence intensity quantified by flow cytometry. (C) Cell density dependence  $\sigma_2$  agonist uptake and cell death. BxPC3 cells were seeded at increasing densities to achieve a range of dividing, subconfluent and quiescent, confluent cultures. The following day, cells were treated with compound 16 ( $25 \text{ nM}$ ) and fluorescence intensity quantitated by flow cytometry. Alternatively, cell were treated with compound 1 or 20 ( $100 \mu\text{M}$ ) for 24 h and viability compared to DMSO control.

dependent/lipid raft pathway has not been previously reported. Interaction and endocytosis of compound 16 through lipid rafts is of note considering that  $\sigma_2$  receptor agonists were initially found to bind to protein constituents of the lipid rafts,<sup>31,32</sup> cholesterol-rich domains in the cell membrane. They form flask-shaped invaginations called caveolae, for the caveolin protein that coats them, and act as platforms for glycoposphatidylinositol-linked protein mediated signaling pathways and internalization of cholesterol.<sup>33</sup> Interest has grown in targeting this pathway in cancer cells, which may have disrupted lipid rafts, contributing to aberrances in pathways implicated in chemoresistance such as the epidermal growth factor receptor and tumor necrosis factor  $\alpha$  receptor.<sup>34</sup>

Therefore, implication of lipid raft disruption in oncology signaling and response to chemotherapy together with the presence of  $\sigma_2$  proteins in lipid rafts suggest that  $\sigma_2$  receptor mediated toxicity and overcame chemoresistance (which has been shown with different  $\sigma_2$  receptor agonists),<sup>23,35</sup> likely involve lipid rafts.

In vitro competition was performed to quantify interaction of compound 16 with  $\sigma_2$  agonists in the live cell. Preloading with 1 or the recently produced  $\sigma_2$  agonist *cis*-1-cyclohexyl-4-[4-(2,6-difluorophenyl)cyclohexyl]piperazine<sup>36</sup> (20) for 45 min prior to addition of compound 16 for 45 min decreased the mean fluorescence intensity of 16 with increasing concentrations of  $\sigma_2$  agonist (Figure 1B). This indicates that the fluorescent

compound functionally competes for localization in the same plane as the parent and analogue compound.

The correlation between the proliferative status of tumors and the expression of the  $\sigma_2$  receptors has been widely demonstrated in different cancer cell lines,<sup>22,37,38</sup> and we have further detailed the expression and apoptosis response in pancreatic cancer cells.<sup>11,39</sup> In this study, we further evaluated the impact of proliferation on  $\sigma_2$  agonist uptake and sensitivity (Figure 1C). To maintain proliferating versus quiescent cell cultures, subcultured cells were seeded at increasing densities in order to achieve subconfluent and confluent cultures, respectively. Compound 16 mean fluorescence at 30 min decreased as cell density increased, in accordance with earlier findings that  $\sigma_2$  receptors are markers of cell proliferation.<sup>40</sup> In addition, the decreased uptake was associated with decreased cell death as the density increased so that the reduction of the antiproliferative activity of  $\sigma_2$  agonists 1 and 20 was likely due to the  $\sigma_2$  reduced presence in nonproliferating cells. Together, these findings show that compound 16 performs biologically as expected for a  $\sigma_2$  ligand and that increased uptake of  $\sigma_2$  agonists by proliferating cells is a critical step for mediating cell death.

Cellular colocalization studies of these fluorescent analogues of 1 were initially screened by epifluorescent microscopy (Supporting Information), and confocal microscopy results were in accordance with those findings (Figure 2). BxPC3 cells were incubated with fluorescent ligand 16 and MitoTracker Red,

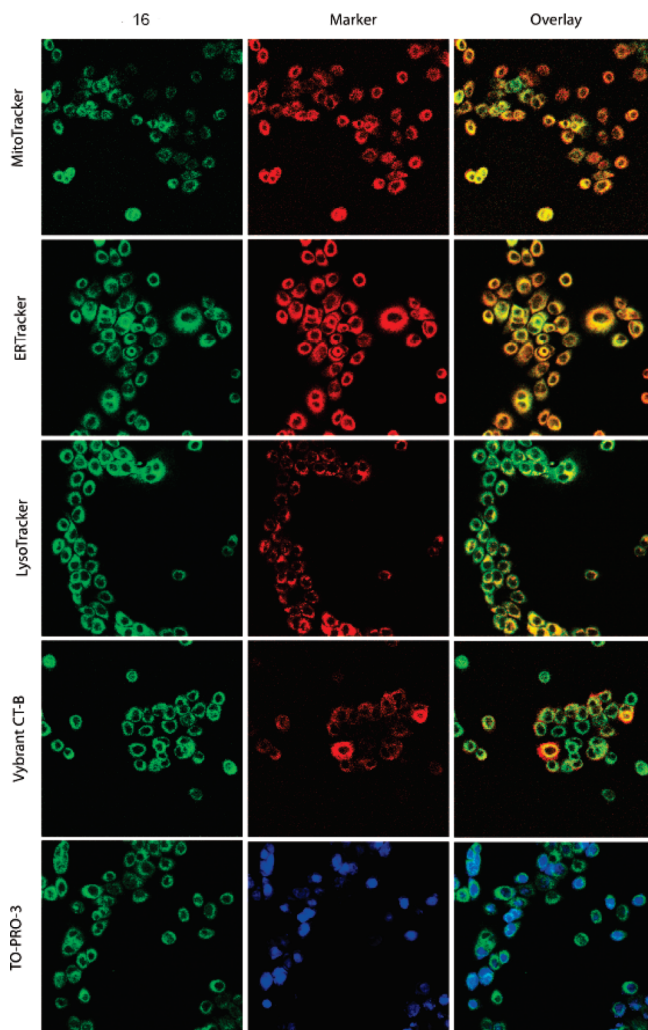


**Figure 2.** Cellular colocalization of **16** with subcellular organelles. BxPC3 pancreatic cancer cells were incubated with **16** and subcellular markers, as described in the Materials and Methods, and imaged by confocal microscopy. **16** is presented as green, organelle markers in red, and overlays in yellow.

ERTracker Red, LysoTracker Red, or Vybrant cholera-toxin B subunit (CT-B), at 37 °C for 30 min prior to fixation and nuclear staining with TO-PRO-3. Compound **16** is found in the membrane fractions of the cell and colocalizes greatest in the endoplasmic reticulum and lysosomes, with moderate colocalization in the mitochondria and the plasma membrane (CT-B). Colocalization in the nucleus was not observed with TO-PRO-3.

## CONCLUSIONS

Fluorescent  $\sigma_2$  ligands were obtained linking dansyl or NBD moieties in two different positions of compound **1** structure. High affinity  $\sigma_2$  ligands were obtained when the fluorescent tag was attached to the tetralin ring through an alkyl linker replacing the methyl in the methoxy function. On the other hand, the approach of attaching a fluorescent tag at the compound **1** cyclohexyl moiety (replaced by a piperidine ring) was unsuccessful, and a dramatic drop in the affinity was recorded. NBD-bearing compounds displayed better fluorescent properties (more convenient  $\lambda_{\text{exc}}$  and  $\lambda_{\text{em}}$  and high fluorescence intensity) than dansyl-bearing compounds, and among them, compound

**16** displayed high  $\sigma_2$  receptor affinity and moderate  $\sigma_1/\sigma_2$  selectivity. Therefore, compound **16** internalization was studied by flow cytometry and by confocal microscopy for colocalization with subcellular organelles in BxPC3 pancreatic tumor cells. The uptake of fluorescent ligand **16** decreased in the presence of nonfluorescent  $\sigma_2$  ligands, showing that fluorescent and nonfluorescent compounds compete for localization in the same plane. Endocytosis inhibitors decreased the uptake of compound **16**, showing that internalization occurs, in part, through endocytotic pathways besides simple membrane diffusion, and that interaction with lipid rafts, which may be able to influence the membrane composition and downstream signaling, takes place so that  $\sigma_2$  receptor mediated toxicity and chemoresistance overcome likely involve lipid rafts. The influence of proliferation, with cell density as a surrogate, on  $\sigma_2$  agonist uptake and sensitivity, was studied and showed that the uptake is higher in proliferating cells, supporting that  $\sigma_2$  receptors are markers of cell proliferation.<sup>37,38</sup> Furthermore, the sensitivity of BxPC3 cells for  $\sigma_2$  agonists decreased, together with the uptake, as the density (i.e., quiescent cells) increased, suggesting that uptake is a critical step for mediating  $\sigma_2$  agonists-dependent cell death. Compound **16** colocalized to the greatest extent in the endoplasmic reticulum and lysosomes, with moderate colocalization in the mitochondria and the plasma membrane but no colocalization in the nucleus was observed, in disagreement with the histone hypothesis which will have to be further analyzed.

All in all, it was demonstrated that the use of fluorescent  $\sigma_2$  ligands may help in clarifying the mechanisms of action of the still enigmatic  $\sigma_2$  receptors. The use of such compounds in different cell lines may contribute to understand the different cell type apoptotic pathways activated by  $\sigma_2$  ligands. Furthermore, a scaffold which appears optimal for inferring high  $\sigma$  receptor affinities was herein produced, and it can be further exploited for obtaining fluorescent molecules with  $\lambda_{\text{exc}}$  and  $\lambda_{\text{em}}$  more shifted toward the near-infrared (NIR) region of the spectrum for a wider application of  $\sigma$  receptor fluorescent ligands in optical molecular imaging techniques.

## MATERIALS AND METHODS

**Chemistry.** Both column chromatography and flash column chromatography were performed with 60 Å pore size silica gel as the stationary phase (1:30 w/w, 63–200  $\mu\text{m}$  particle size, from ICN, and 1:15 w/w, 15–40  $\mu\text{m}$  particle size, from Merck, respectively). Melting points were determined in open capillaries on a Gallenkamp electrothermal apparatus. Purity of tested compounds was established by combustion analysis, confirming a purity  $\geq 95\%$ . Elemental analyses (C, H, N) were performed on a Eurovector Euro EA 3000 analyzer; the analytical results were within  $\pm 0.4\%$  of the theoretical values unless otherwise indicated.  $^1\text{H}$  NMR spectra were recorded on a Mercury Varian 300 MHz using  $\text{CDCl}_3$  as solvent. The following data were reported: chemical shift ( $\delta$ ) in ppm, multiplicity (s = singlet, d = doublet, t = triplet, m = multiplet), integration, and coupling constant(s) in hertz. Recording of mass spectra was done on an Agilent 6890–5973 MSD gas chromatograph/mass spectrometer and on an Agilent 1100 series LC-MSD trap system VL mass spectrometer; only significant  $m/z$  peaks, with their percentage of relative intensity in parentheses, are reported. Chemicals were from Aldrich and Across and were used without any further purification.

**6-(1,4-Dioxo-8-azaspiro[4.5]dec-8-yl)hexanenitrile (2).** A mixture of 1,4-dioxo-8-azaspiro[4.5]decane (0.72 mL, 5.6 mmol), triethylamine (0.78 mL, 5.6 mmol), and 6-bromohexanenitrile (0.74 mL, 5.6 mmol) in  $\text{CH}_2\text{Cl}_2$  was stirred at room temperature.

The reaction mixture was washed with H<sub>2</sub>O, and the separated organic layer was concentrated under reduced pressure to give a crude mixture, which was purified by column chromatography with CH<sub>2</sub>Cl<sub>2</sub>/MeOH (95:5) as eluent, to afford the target compound as a pale-yellow oil (1.16 g, 87% yield). <sup>1</sup>H NMR δ 1.42–1.56 (m, 2H), 1.64–1.84 (m, 4H), 1.86–2.10 (m, 4H), 2.36 (t, 2H, *J* = 7.2 Hz), 2.68 (t, 2H, *J* = 8 Hz), 2.80–3.00 (m, 4H), 4.00 (s, 4H). GC-MS *m/z* 239 (M<sup>+</sup> + 1, 1), 238 (M<sup>+</sup>, 3), 156 (100).

**N-[6-(1,4-Dioxo-8-aza-spiro[4.5]dec-8-yl)hexyl]acetamide (3).** A solution of the nitrile **2** (1.0 g, 4.2 mmol) in anhydrous Et<sub>2</sub>O (25 mL) was added in a dropwise manner to a suspension of LiAlH<sub>4</sub> (0.32 g, 8.4 mmol) in the same solvent kept under N<sub>2</sub> at 0 °C. The mixture was stirred at 0 °C for 45 min and then at room temperature overnight. H<sub>2</sub>O was carefully added into the reaction pot, and the obtained mixture was filtered on Celite pad and the filtrate evaporated under reduced pressure to give the corresponding amine as a pale-yellow gummy solid (1.0 g, 99% yield). GC-MS *m/z* 242 (M<sup>+</sup>, 1), 156 (100). Such amine (1.0 g, 4.2 mmol) was dissolved in anhydrous CH<sub>2</sub>Cl<sub>2</sub> (40 mL) and added with triethylamine (1.2 mL, 8.6 mmol). Acetyl chloride (0.45 mL, 6.4 mmol) was then dropped at 0 °C, under N<sub>2</sub>. The mixture was stirred at room temperature for 3 h and then treated with NaHCO<sub>3</sub> (satd solution 20 mL), and extracted with CH<sub>2</sub>Cl<sub>2</sub> (3 × 20 mL). The organic layers collected were dried (Na<sub>2</sub>SO<sub>4</sub>) and concentrated under reduced pressure to give a crude mixture, which was purified by column chromatography with CH<sub>2</sub>Cl<sub>2</sub>/MeOH (9:1) as eluent to yield title compound as a pale-yellow oil (0.78 g, 66% yield). GC-MS *m/z* 284 (M<sup>+</sup>, 1), 156 (100).

**N-[6-(4-Oxopiperidino)hexyl]acetamide (4).** To a solution of amide **3** (0.32 g, 1.13 mmol) in acetone, 2 N HCl (37 mL) was added and the mixture was heated at reflux for 1 h followed by 1 h at room temperature. The solvent was removed under reduced pressure, and conc NaOH was added to obtain an alkaline pH. The aqueous phase was extracted with AcOEt (3 × 15 mL), and the organic layers collected and dried (Na<sub>2</sub>SO<sub>4</sub>) and evaporated under reduced pressure to afford the target compound as a yellow oil (0.17 g, 63% yield), which was used for the next step without further purification. <sup>1</sup>H NMR δ 1.42–1.84 (m, 8H), 2.10–2.68 (s+m, 13H), 2.90–3.10 (m, 2H), 5.10 (broad s, 1H). GC-MS *m/z* 240 (M<sup>+</sup>, 1), 112 (100).

**6-[4-[4-[3-(5-Methoxy-1,2,3,4-tetrahydronaphthalen-1-yl)propyl]piperazin-1-yl]piperidino]hexylamine (6).** The piperidine **4** (0.16 g, 0.67 mmol) and piperazine **5** (0.19 g, 0.68 mmol) were reacted with ZnCl<sub>2</sub> (0.05 g, 0.39 mmol) and NaCNBH<sub>3</sub> (0.044 g, 0.70 mmol) in 2-propanol (20 mL). The mixture was stirred for 48 h at room temperature. Then, the reaction mixture was evaporated to dryness, and the residue was diluted with 2 N NaOH and extracted with AcOEt. The organic layers were washed with brine, dried (Na<sub>2</sub>SO<sub>4</sub>), and then concentrated under reduced pressure to give a crude residue, which was purified by column chromatography with CH<sub>2</sub>Cl<sub>2</sub>/MeOH (8:2) as eluent to afford the intermediate *N*-acetyl derivative of compound **6** as a white solid (0.13 g, 39% yield). <sup>1</sup>H NMR δ 1.20–2.00 (m, 23H), 2.20–2.40 (m, 6H), 2.45–3.00 (m, 14H), 3.20 (m, 2H), 3.80 (s, 3H), 5.45 (broad s, 1H), 6.65 (d, 1H, *J* = 7.7 Hz), 6.80 (d, 1H, *J* = 7.7 Hz), 7.08 (t, 1H, *J* = 7.9 Hz). LC-MS (ESI<sup>+</sup>) *m/z* 513 [M + H]<sup>+</sup>, 535 [M + Na]<sup>+</sup>. Such intermediate acetamide (0.22 g, 0.44 mmol) was refluxed in 3N HCl (6.5 mL) for 4 h. After cooling, the mixture was made alkaline with K<sub>2</sub>CO<sub>3</sub> (satd solution, 10 mL) and extracted with CH<sub>2</sub>Cl<sub>2</sub> (3 × 10 mL). The collected organic layers were dried (Na<sub>2</sub>SO<sub>4</sub>), and the solvent was evaporated to produce a brown semisolid (0.20 g, 99% yield), which was used for the next step without any further purification. <sup>1</sup>H NMR δ 1.20–2.00 (m, 20H), 2.20–2.80 (m, 19H), 2.85–3.05 (m, 3H), 3.80 (s, 3H), 5.45 (broad s, 2H, D<sub>2</sub>O exchanged), 6.65 (d, 1H, *J* = 7.7 Hz), 6.80 (d, 1H, *J* = 7.7 Hz), 7.08 (t, 1H, *J* = 7.9 Hz). LC-MS (ESI<sup>+</sup>) *m/z* 471 [M + H]<sup>+</sup>.

**2-(6-[5-[3-(4-Cyclohexylpiperazin-1-yl)propyl]-5,6,7,8-tetrahydronaphthalen-1-yloxy]hexyl)isoindole-1,3-dione (11).** A grain of NaI, K<sub>2</sub>CO<sub>3</sub> (0.14 g, 1.0 mmol), and phthalimide **9** (0.29 g, 1.0 mmol) were added to a solution of phenol **10** (0.26 g, 0.74 mmol) in DMF (5 mL), and the reaction mixture was heated at 100 °C for 18 h. After cooling, the solvent was removed under reduced pressure, and then H<sub>2</sub>O (5 mL) was added to the residue and the mixture was extracted with AcOEt (3 × 10 mL). The crude was purified by flash chromatography with ethyl acetate/CH<sub>2</sub>Cl<sub>2</sub> (6:4) as eluent to give compound **11** as a yellow oil (0.094 g, 16% yield). <sup>1</sup>H NMR δ 1.21–1.97 (m, 26H), 2.10–2.95 (m, 14H), 3.69 (t, 2H, *J* = 7.2 Hz), 3.90 (m, 2H), 6.57–7.07 (m, 3H), 7.60–7.86 (m, 4H). LC-MS (ESI<sup>+</sup>) *m/z* 586 [M + H]<sup>+</sup>, 608 [M + Na]<sup>+</sup>.

**2-[2-[5-[3-(4-Cyclohexylpiperazin-1-yl)propyl]-5,6,7,8-tetrahydronaphthalen-1-yloxy]ethoxy]ethanol (12).** To a solution of phenol **10** (0.14 g, 0.4 mmol) in DMF (5 mL), a grain of NaI, K<sub>2</sub>CO<sub>3</sub> (0.06 g, 0.5 mmol), and 2-(2-chloroethoxy)ethanol (0.05 mL, 0.5 mmol) were added, and the reaction mixture was heated at 120 °C for 18 h. After cooling, the solvent was evaporated under reduced pressure, and then water was added to the residue. The mixture was extracted with AcOEt (3 × 5 mL), and the collected organic layers collected were dried (Na<sub>2</sub>SO<sub>4</sub>) and evaporated to afford a crude, which was purified by flash chromatography with AcOEt/CH<sub>2</sub>Cl<sub>2</sub> (7:3) as eluent to give the target compound **12** as a yellow oil (0.11 g, 62% yield). <sup>1</sup>H NMR δ 1.00–1.40 (m, 6H), 1.40–2.00 (m, 12H), 2.40–3.20 (m, 15H), 3.65–3.80 (m, 4H), 3.86–3.90 (m, 2H), 4.06–4.12 (m, 2H), 6.65–7.05 (m, 3H). GC-MS *m/z* 445 (M<sup>+</sup> + 1, 5), 444 (M<sup>+</sup>, 22), 181 (100). LC-MS (ESI<sup>+</sup>) *m/z* 445 [M + H]<sup>+</sup>, 467 [M + Na]<sup>+</sup>.

**2-[2-[2-[5-[3-(4-Cyclohexylpiperazin-1-yl)propyl]-5,6,7,8-tetrahydronaphthalen-1-yloxy]ethoxy]ethyl]isoindole-1,3-dione (13).** To a stirred solution of alcohol **12** (0.12 g, 0.27 mmol) in dry THF (10 mL) kept under N<sub>2</sub>, triphenylphosphine (0.12 g, 0.46 mmol), phthalimide (0.069 g, 0.47 mmol), and DIAD (0.12 mL, 0.60 mmol) were added, and the mixture was stirred at room temperature for 18 h. Then the solvent was evaporated under reduced pressure, and the resulting residue was treated with H<sub>2</sub>O and the aqueous layer was extracted with AcOEt (3 × 20 mL). The combined organic layers were dried (Na<sub>2</sub>SO<sub>4</sub>) and concentrated under reduced pressure to give a crude residue, which was purified by column chromatography using CH<sub>2</sub>Cl<sub>2</sub>/MeOH (95:5) as eluent, to afford the target compound as a yellow oil (0.10 g, 65% yield). LC-MS (ESI<sup>+</sup>) *m/z* 574 [M + H]<sup>+</sup>, 596 [M + Na]<sup>+</sup>.

**General Procedure for the Synthesis of 6-[1-[3-(4-Cyclohexylpiperazin-1-yl)-propyl]-1,2,3,4-tetrahydronaphthalen-5-yloxy]hexylamine (14) and 2-[2-[1-[3-(4-Cyclohexylpiperazin-1-yl)propyl]-1,2,3,4-tetrahydronaphthalen-5-yloxy]ethoxy]ethylamine (15).** Hydrazine hydrate 50% (0.085 mL, 0.85 mmol) was added to a solution of either **11** or **13** (0.29 mmol) in methanol (3 mL), and the reaction mixture was stirred at room temperature for 30 min. Then 1.5 N HCl (1.2 mL) was then added, and the mixture was stirred for further 12 h. Then 3 N HCl was added until a pH < 2 was obtained, and the mixture was heated at reflux for 30 min. After cooling down to room temperature, the mixture was filtered, the solid residue was washed with cold MeOH and with Et<sub>2</sub>O, and dried under vacuum. The white solid obtained was made free base with alkaline treatment to afford the target compound as a pale-yellow oil (70% yield).

**6-[1-[3-(4-Cyclohexylpiperazin-1-yl)propyl]-1,2,3,4-tetrahydronaphthalen-5-yloxy]hexylamine (14).** <sup>1</sup>H NMR δ 1.00–1.30 (m, 5H), 1.40–2.00 (m, 23H), 2.20–2.80 (m, 16H), 3.90 (t, 2H, *J* = 6.0 Hz), 6.60 (d, 1H, *J* = 7.9 Hz), 6.75 (d, 1H, *J* = 7.7 Hz), 7.05 (t, 1H, *J* = 7.9 Hz). LC-MS (ESI<sup>+</sup>) *m/z* 456 [M + H]<sup>+</sup>.

**2-[2-[1-[3-(4-Cyclohexylpiperazin-1-yl)propyl]-1,2,3,4-tetrahydronaphthalen-5-yloxy]ethoxy]ethylamine (15).** <sup>1</sup>H NMR δ 1.05–1.50

(m, 6H), 1.60–2.10 (m, 12H), 2.40–3.20 (m, 18H), 3.65–3.90 (m, 6H), 6.65–7.05 (m, 3H). LC-MS (ESI<sup>+</sup>) *m/z* 444 [M + H]<sup>+</sup>, 466 [M + Na]<sup>+</sup>.

**General Procedure for the Synthesis of Final Compounds 7, 16, 17.** 4-Chloro-7-nitro-2,1,3-benzoxadiazole (NBD-Cl, 1.0 mmol) was dissolved in absolute EtOH (15 mL) and added in a dropwise manner to one among amines **6**, **14**, or **15** (1.0 mmol) dissolved in the same solvent (15 mL). The mixture was stirred for 1.5 h at room temperature. Then the reaction mixture was filtered and the filtrate evaporated under reduced pressure.

6-[4-[4-[3-(5-Methoxy-1,2,3,4-tetrahydronaphthalen-1-yl)propyl]piperazin-1-yl]piperidino]-N-(7-nitro-2,1,3-benzoxadiazol-4-yl)hexanamine (**7**). The crude semisolid was purified by column chromatography with AcOEt/MeOH (7:3) as eluent to give the final compound **7** as an orange semisolid (0.26 g, 42% yield). <sup>1</sup>H NMR δ 1.20–2.20 (m, 21H), 2.25–2.35 (m, 8H), 2.45–2.80 (m, 11H), 3.00–3.10 (m, 2H), 3.20–3.40 (broad s, 1H), 3.80 (s, 3H), 6.18 (d, 1H, *J* = 8.5 Hz), 6.60 (d, 1H, *J* = 7.7 Hz), 6.80 (d, 1H, *J* = 7.7 Hz), 7.05 (t, 1H, *J* = 7.9 Hz), 8.50 (d, 1H, *J* = 8.5 Hz). LC-MS (ESI<sup>+</sup>) *m/z* 634 [M + H]<sup>+</sup>, 656 [M + Na]<sup>+</sup>. Anal. (C<sub>35</sub>H<sub>51</sub>N<sub>7</sub>O<sub>4</sub> · 3.8HCl) C, H, N.

6-[5-[3-(4-Cyclohexylpiperazin-1-yl)propyl]-5,6,7,8-tetrahydronaphthalen-5-yloxy]-N-(7-nitro-2,1,3-benzoxadiazol-4-yl)hexanamine (**16**). The crude semisolid was purified by column chromatography using CH<sub>2</sub>Cl<sub>2</sub>/MeOH (99:1) as eluent to give the target compound **16** as a brown oil (0.37 g, 60% yield). <sup>1</sup>H NMR δ 1.00–1.40 (m, 10H), 1.50–2.00 (m, 16H), 2.18–2.80 (m, 13H), 3.45–3.55 (m, 3H), 3.94 (t, 2H, *J* = 6.0 Hz), 6.17 (d, 1H, *J* = 8.5 Hz), 6.20–6.30 (broad s, 1H, D<sub>2</sub>O exchanged), 6.60 (d, 1H, *J* = 7.7 Hz), 6.78 (d, 1H, *J* = 7.7 Hz), 7.05 (t, 1H, *J* = 7.9 Hz), 8.50 (d, 1H, *J* = 8.5 Hz). LC-MS (ESI<sup>+</sup>) *m/z* 617 [M – H]<sup>–</sup>. Anal. (C<sub>35</sub>H<sub>50</sub>N<sub>6</sub>O<sub>4</sub> · 3HCl · 5/4H<sub>2</sub>O) C, H, N.

2-[2-[5-[3-(4-Cyclohexylpiperazin-1-yl)propyl]-5,6,7,8-tetrahydronaphthalen-1-yloxy]ethoxy]-N-(7-nitro-2,1,3-benzoxadiazol-4-yl)ethanamine (**17**). The crude semisolid was purified by column chromatography using CH<sub>2</sub>Cl<sub>2</sub>/MeOH (99:1) as eluent to give the final compound **17** as a brown oil (0.37 g, 62% yield). <sup>1</sup>H NMR δ 1.40–2.20 (m, 18H), 2.25–2.80 (m, 14H), 3.50–3.75 (m, 3H), 3.85–4.00 (m, 4H), 4.08–4.15 (m, 2H), 6.17 (d, 1H, *J* = 8.5 Hz), 6.60 (d, 1H, *J* = 7.7 Hz), 6.80 (d, 1H, *J* = 7.7 Hz), 7.05 (t, 1H, *J* = 7.9 Hz), 8.45 (d, 1H, *J* = 8.5 Hz). LC-MS (ESI<sup>+</sup>) *m/z* 607 [M + H]<sup>+</sup>. Anal. (C<sub>33</sub>H<sub>46</sub>N<sub>6</sub>O<sub>5</sub> · 3HCl) C, H, N.

**General Procedure for the Synthesis of Final Compounds 8, 18, 19.** A solution of 5-(dimethylamino)naphthalene-1-sulfonyl chloride (dansyl chloride) (0.21 g, 0.8 mmol) in anhydrous CH<sub>2</sub>Cl<sub>2</sub> (15 mL) was added in a dropwise manner to one among amines **6**, **14**, or **15** (1.0 mmol) dissolved in the same solvent (15 mL). The mixture was stirred at room temperature for 18 h. Then, the reaction mixture was washed with H<sub>2</sub>O (2 × 30 mL) and the organic phases were collected, dried (Na<sub>2</sub>SO<sub>4</sub>), and evaporated under reduced pressure to afford a crude residue, which was purified as described below.

5-Dimethylaonaphthalene-1-sulfonic acid 6-[4-[4-[3-(5-methoxy-1,2,3,4-tetrahydronaphthalen-1-yl)propyl]piperazin-1-yl]piperidino]hexanamide (**8**). The crude semisolid was purified by column chromatography using CHCl<sub>3</sub>/MeOH (9:1) as eluent to give the target compound as a green oil (0.29 g, 42% yield). <sup>1</sup>H NMR δ 1.04–1.45 (m, 8H), 1.50–2.10 (m, 12H), 2.20–2.40 (m, 6H), 2.45–2.80 (m, 11H), 2.92–3.02 (m, 11H), 3.80 (s, 3H), 4.90–5.00 (m, 1H, D<sub>2</sub>O exchanged), 6.63 (d, 1H, *J* = 7.7 Hz), 6.78 (d, 1H, *J* = 7.7 Hz), 7.08 (t, 1H, *J* = 7.7 Hz), 7.18 (d, 1H, *J* = 7.4 Hz), 7.50–7.60 (m, 2H), 8.22 (d, 1H, *J* = 7.4 Hz), 8.30 (d, 1H, *J* = 7.4 Hz), 8.55 (d, 1H, *J* = 7.4 Hz). LC-MS (ESI<sup>+</sup>) *m/z* 704 [M + H]<sup>+</sup>. Anal. (C<sub>41</sub>H<sub>61</sub>N<sub>5</sub>O<sub>3</sub>S · 4HCl · 2H<sub>2</sub>O) C, H, N.

5-Dimethylaonaphthalene-1-sulfonic acid 6-[5-[3-(4-cyclohexylpiperazin-1-yl)propyl]-5,6,7,8-tetrahydronaphthalen-1-yloxy]hexanamide (**18**). The crude semisolid was purified by column chromatography

using CH<sub>2</sub>Cl<sub>2</sub>/MeOH (97:3) as eluent to give the target compound **18** as a pale-green oil (0.33 g, 48% yield). <sup>1</sup>H NMR δ 1.00–1.90 (m, 24H), 2.00–2.20 (m, 2H), 2.40–3.10 (m, 22H), 3.80 (t, 2H, *J* = 6 Hz), 4.70–4.80 (m, 1H, D<sub>2</sub>O exchanged), 6.55 (d, 1H, *J* = 7.9 Hz), 6.73 (d, 1H, *J* = 7.7 Hz), 7.00–7.05 (m, 1H), 7.20 (d, 1H, *J* = 7.9 Hz), 7.50–7.60 (m, 2H), 8.20–8.40 (m, 2H), 8.51 (d, 1H, *J* = 8.5 Hz). LC-MS (ESI<sup>+</sup>) *m/z* 689 [M + H]<sup>+</sup>. Anal. (C<sub>41</sub>H<sub>60</sub>N<sub>4</sub>O<sub>3</sub>S · 3HCl · 3/2H<sub>2</sub>O) C, H, N.

5-Dimethylaonaphthalene-1-sulfonic acid 2-[2-[5-[3-(4-cyclohexylpiperazin-1-yl)propyl]-5,6,7,8-tetrahydronaphthalen-5-yloxy]ethoxy]ethanamide (**19**). The crude semisolid was purified by column chromatography using CH<sub>2</sub>Cl<sub>2</sub>/MeOH (98:2) as eluent to give the target compound as a pale-green oil (0.47 g, 70% yield). <sup>1</sup>H NMR δ 1.00–2.30 (m, 18H), 2.50–3.40 (m, 22H), 3.45 (t, 2H, *J* = 5 Hz), 3.55 (t, 2H, *J* = 6 Hz), 3.90 (t, 2H, *J* = 6 Hz), 5.20–5.30 (m, 1H, D<sub>2</sub>O exchanged), 6.55 (d, 1H, *J* = 7.9 Hz), 6.76 (d, 1H, *J* = 7.7 Hz), 7.00–7.10 (m, 1H), 7.14 (d, 1H, *J* = 7.9 Hz), 7.40–7.54 (m, 2H), 8.20–8.26 (m, 2H), 8.51 (d, 1H, *J* = 8.5 Hz). LC-MS (ESI<sup>+</sup>) *m/z* 677 [M + H]<sup>+</sup>. Anal. (C<sub>39</sub>H<sub>56</sub>N<sub>4</sub>O<sub>4</sub>S · 3HCl) C, H, N.

**Fluorescence Spectroscopy and Molar Extinction Coefficient.** Emission spectra of compounds **7**, **8**, and **16–19** were determined in EtOH, CHCl<sub>3</sub>, and in PBS buffer solution. In all experiments, the excitation and the emission bandpass was set at 10 nm. The emission spectra were obtained from 300 to 700 nm, with excitation set at the appropriate excitation wavelength. The excitation spectra of compounds **8**, **18**, and **19** were obtained from 250 to 450 nm, with the emission being recorded at the appropriate wavelength. The excitation spectra of compounds **7**, **16**, and **17** were obtained from 300 to 550 nm, with the emission being recorded at the appropriate wavelength. Fluorescence quantum yields were calculated with respect to quinine sulfate (Fluka) in 0.5 M H<sub>2</sub>SO<sub>4</sub> as a standard ( $\Phi = 0.546$ ).<sup>41</sup> Solutions of both the sample and the reference were prepared from original solutions diluted with the appropriate solvent so that absorbance was below 0.2 at the same excitation wavelength (347 nm). Fluorescence measurements were carried out for each solution with the same instrument parameters, and the fluorescence spectra were corrected for instrumental response before integration. The quantum yield for each sample was calculated according to the following equation:<sup>42</sup>

$$\Phi_x = \Phi_s (A_s/A_x) (F_x/F_s) (n_x/n_s)^2$$

where  $\Phi$  is the emission quantum yield, *A* is the absorbance at the excitation wavelength, *F* is the area under the corrected emission curve, *n* is the refractive index of the solvent for the sample (*X*) and the standard (*S*). Absorption spectra were recorded with a PerkinElmer UV–vis-NIR spectrophotometer, and fluorescence spectra were obtained with a PerkinElmer LS55 spectrofluorometer. Molar extinction coefficients ( $\epsilon$ ) were determined for each final compound (**7**, **8**, **16–19**) dissolved in EtOH, with concentration ranging from 1 to 100  $\mu$ M and absorbance spectra recorded from 200 to 600 nm in standard quartz cuvettes.  $\epsilon$  values were determined by fitting the Beer's law:  $A = \epsilon \times c \times d$  where (*A*) is the absorbance at the  $\lambda_{exc}$ ; (*c*) is the molar concentration of the solution, and (*d*) was the optical path length (*d* = 1 cm). Measurements were repeated twice.

**Biological Methods and Materials.** *Radioligand Binding Assays.* All the procedures for the binding assays were previously described.  $\sigma_1$  and  $\sigma_2$  receptor binding were carried out according to Matsumoto et al.<sup>43</sup> [<sup>3</sup>H]-DTG (30 Ci/mmol) and (+)-[<sup>3</sup>H]-pentazocine (34 Ci/mmol) were purchased from PerkinElmer Life Sciences (Zaventem, Belgium). DTG was purchased from Tocris Cookson Ltd., UK. (+)-Pentazocine was obtained from Sigma-Aldrich-RBI srl (Milan, Italy). Male Dunkin guinea pigs and Wistar Hannover rats (250–300 g) were from Harlan, Italy. The specific radioligands and tissue sources were respectively: (a)  $\sigma_1$  receptor, (+)-[<sup>3</sup>H]-pentazocine (+)-[2S-(2 $\alpha$ ,6 $\alpha$ ,11-R)]-1,2,3,4,5,6-hexahydro-6,11-dimethyl-3-(3-methyl-2-butenyl)-2,6-methano-3-benzazocine-8-ol, guinea pig brain membranes without cerebellum;

(b)  $\sigma_2$  receptor, [ $^3\text{H}$ ]-DTG in the presence of 1  $\mu\text{M}$  (+)-pentazocine to mask  $\sigma_1$  receptors, rat liver membranes. The following compounds were used to define the specific binding reported in parentheses: (a) (+)-pentazocine (73–87%), (b) DTG (85–96%). Concentrations required to inhibit 50% of radioligand specific binding ( $\text{IC}_{50}$ ) were determined by using six–nine different concentrations of the drug studied in two or three experiments with samples in duplicate. Scatchard parameters ( $K_d$  and  $B_{\text{max}}$ ) and apparent inhibition constants ( $K_i$ ) values were determined by nonlinear curve fitting by using the Prism, version 3.0, GraphPad software.<sup>44</sup>

**Cell Culture.** BxPC3 pancreatic cancer cells were maintained in Roswell Park Memorial Institute (RPMI) media (GIBCO) supplemented with L-glutamine (2 mM), 4-(2-hydroxyethyl)-1-piperazineethanesulfonic acid (HEPES) (1 mM), pyruvate (1 mM), sodium bicarbonate (0.075% w/v), penicillin, and streptomycin (100 IU/mL), amphotericin (0.25  $\mu\text{g}/\text{mL}$ ), and 10% fetal bovine serum (Atlanta Biologicals, Lawrenceville, GA). Cells were seeded at a density of  $2 \times 10^5/\text{mL}$  unless otherwise stated and maintained in a humidified atmosphere of 5%  $\text{CO}_2$  at 37 °C.

**Confocal Microscopy.** For subcellular compartmentalization, cells grown on glass coverslips were incubated with compound **16** (100 nM) and either ERTracker Red (1  $\mu\text{M}$ ), MitoTracker Red (100 nM), or LysoTracker Red (50 nM) for 30 min at 37 °C. The plasma membrane was visualized using the Vybrant Alexa Fluor 594 lipid raft labeling kit as directed by the manufacturer. All reagents were obtained from Molecular Probes. Cells were washed with PBS and fixed in 2% paraformaldehyde for 30 min at 37 °C prior to additional washing and mounting to a slide with ProLong Gold antifade reagent. Imaging was performed on a Carl Zeiss Axiovert 100 inverted microscope, fitted with LSM 510 laser scanning microscope camera and software. Images were collected with filter bandwidths corresponding to 505–530 nm for green, 560–615 nm for red, and >650 nm for far red, with 4 scans over 11.8 s.

**Internalization of Compound 16 by Flow Cytometry.** To quantify internalization of compound **16**, cells were pretreated with the endocytosis inhibitors phenylarsine oxide (10  $\mu\text{M}$ ) or Filipin III (5  $\mu\text{g}/\text{mL}$ ) for 60 min at 37 °C prior to washing and resuspension in cell media. Compound **16** (25 nM) was added and the mean fluorescence (FL1) quantified with a FACSCalibur flow cytometer (BD Biosciences, San Jose, CA) with kinetic readings over a time period of 60 min. To detect competition of compound **16** with parent and analogous compounds, BxPC3 cells were treated with compounds **1** or **20** at increasing concentrations for 45 min prior to replacement with compound **16** (25 nM) for 45 min at 37 °C and fluorescence intensity quantified by flow cytometry. To deter the influence of cell proliferation by increasing the cell seeding density, BxPC3 cells were seeded at increasing concentrations, and the following day, cells were treated with compound **16** (25 nM) for 30 min at 37 °C and fluorescence intensity quantified by flow cytometry.

**Cell Viability.** Subcultured BxPC3 cells were seeded at increasing densities from  $1 \times 10^5$  to  $9 \times 10^5$  into 96-well clear-bottom plates 24 h prior to treatment with compounds **1** or **20** (100  $\mu\text{M}$ ). Then 18 h later, cells were washed with PBS, fixed with 4% paraformaldehyde for 30 min at 37 °C, and stained with crystal violet for 15 min at 37 °C. Cells were then washed with PBS and cell density detected with a Bio-Rad Laboratories ChemiDoc XRS+ Imager and quantified with Quantity One software. Viability is represented as the percent density of  $\sigma_2$  agonist treated cells compared to those treated with DMSO vehicle.

## ■ ASSOCIATED CONTENT

Supporting Information. Elemental analyses of the novel end products; formulas, melting points of hydrochloride salts; fluorescence microscopy images taken with compound **16** and subcellular organelles trackers. This material is available free of charge via the Internet at <http://pubs.acs.org>.

## ■ AUTHOR INFORMATION

### Corresponding Author

\*Phone: +39-080-5442748. Fax: +39-080-5442231. E-mail: [abate@farmchim.uniba.it](mailto:abate@farmchim.uniba.it)

## ■ ACKNOWLEDGMENT

This project was partially financed by Veterans Administration Merit Award (project 1136919) (W.G.H.), American Cancer Society (project MRSG08019-01CDD) (W.G.H.), and National Institutes of Health T32 Training Grant (project 5T32CA009621-22) (J.R.H.).

## ■ ABBREVIATIONS USED

NBD, 7-nitro-1,2,3-benzoxadiazole; ER, endoplasmic reticulum; DIAD, diisopropylazodicarboxylate; SAfIR, structure–affinity relationship; PBS, phosphate buffered saline; PAO, phenylarsine oxide; UV, ultraviolet; NIR, near-infrared; DMSO, dimethyl sulfoxide

## ■ REFERENCES

- (1) Quirion, R.; Bowen, W. D.; Itzhak, Y.; Junien, J. L.; Musachio, J. M.; Rothman, R. B.; Su, T.-P.; Tam, S. W.; Taylor, D. P. A proposal for the classification of sigma binding sites. *Trends Pharmacol. Sci.* **1992**, *13*, 85–86.
- (2) Hanner, M.; Moebius, F. F.; Flandorfer, A.; Knaus, H. G.; Striessnig, J. M.; Kempner, E.; Glossmann, H. Purification, molecular cloning, and expression of the mammalian sigma1-binding site. *Proc. Natl. Acad. Sci. U.S.A.* **1996**, *93*, 8072–8077.
- (3) Tsai, S.-Y.; Hayashi, T.; Mori, T.; Su, T.-P. Sigma-1 receptor chaperones and diseases. *Cent. Nerv. Syst. Agents Med. Chem.* **2009**, *9*, 184–189.
- (4) Cobos, E. J.; Entrena, J. M.; Nieto, F. R.; Cendan, C. M.; Del Pozo, E. Pharmacology and therapeutic potential of sigma<sub>1</sub> receptor ligands. *Curr. Neuropharmacol.* **2008**, *6*, 344–366.
- (5) Skuza, G. Potential antidepressant activity of sigma ligands. *Pol. J. Pharm.* **2003**, *55*, 923–934.
- (6) Skuza, G.; Rogoz, Z. Effect of BD1047, a sigma<sub>1</sub> receptor antagonist, in the animal models predictive of antipsychotic activity. *Pharmacol. Rep.* **2006**, *58*, 626–635.
- (7) Jansen, K. L.; Faull, R. L.; Storey, P.; Leslie, R. A. Loss of sigma binding sites in the CA1 area of the anterior hippocampus in Alzheimer's disease correlates with CA1 pyramidal cell loss. *Brain Res.* **1993**, *623*, 299–302.
- (8) Mishina, M.; Ishiwata, K.; Ishii, K.; Kitamura, S.; Kimura, Y.; Kawamura, K.; Oda, K.; Sasaki, T.; Sakayori, O.; Hamamoto, M.; Kobayashi, S.; Katayama, Y. Function of sigma<sub>1</sub> receptors in Parkinson's disease. *Acta Neurol. Scand.* **2005**, *112*, 103–107.
- (9) Mishina, M.; Ohyama, M.; Ishii, K.; Kitamura, S.; Kimura, Y.; Oda, K.; Kawamura, K.; Sasaki, T.; Kobayashi, S.; Katayama, Y.; Ishiwata, K. Low density of sigma<sub>1</sub> receptors in early Alzheimer's disease. *Ann. Nucl. Med.* **2008**, *22*, 151–156.
- (10) Matsumoto, R. R.; Gilmore, D. L.; Pouw, B.; Bowen, W. D.; Williams, W.; Kausar, A.; Coop, A. Novel analogs of the  $\sigma$  receptor ligand BD1008 attenuate cocaine induced toxicity in mice. *Eur. J. Pharmacol.* **2004**, *492*, 21–26.
- (11) Kashiwagi, H.; McDunn, J. E.; Simon, P. O.; Goedegebuure, P. S.; Xu, J.; Jones, L.; Chang, K.; Johnston, F.; Trinkaus, K.; Hotchkiss, R. S.; Mach, R. H.; Hawkins, W. G. Selective sigma-2 ligands preferentially bind to pancreatic adenocarcinomas: applications in diagnostic imaging and therapy. *Mol. Cancer* **2007**, *6*, doi: 10.1186/1476-4598-6-48.
- (12) Crawford, K. W.; Bowen, W. D. Sigma-2 receptor agonists activate a novel apoptotic pathway and potentiate antineoplastic drugs in breast tumor cell lines. *Cancer Res.* **2002**, *62*, 313–322.

- (13) Ostefeld, M. S.; Fehrenbacher, N.; Hover-Hansen, M.; Thomssen, C.; Farkas, T.; Jaattela, M. Effective tumor cell death by sigma-2 receptor ligand siramesine involves lysosomal leakage and oxidative stress. *Cancer Res.* **2005**, *65*, 8975–8983.
- (14) van Waarde, A.; Rybczynska, A. A.; Ramakrishnan, N.; Ishiwata, K.; Elsinga, P. H.; Dierckx, R. A. Sigma receptors in oncology: therapeutic and diagnostic applications of sigma ligands. *Curr. Pharm. Des.* **2010**, *16*, 3519–3537.
- (15) Megalizzi, V.; Le Mercier, M.; Decaestecker, C. Sigma receptors and their ligands in cancer biology: overview and new perspectives for cancer therapy. *Med. Res. Rev.* **2011**, *31*, doi: 10.1002/med.20218
- (16) Phase I Clinical Trial. ClinicalTrials.gov Identifier: NCT0-0968656. Assessment of Cellular Proliferation in Tumors by Positron Emission Tomography (PET) Using [<sup>18</sup>F]ISO-1 (FISO PET/CT).
- (17) Colabufo, N. A.; Berardi, F.; Abate, C.; Contino, M.; Niso, M.; Perrone, R. Is the  $\sigma_2$  receptor a histone binding protein? *J. Med. Chem.* **2006**, *49*, 4153–4158.
- (18) Berardi, F.; Abate, C.; Ferorelli, S.; Colabufo, N. A.; Perrone, R. 1-Cyclohexylpiperazine and 3,3-dimethylpiperidine derivatives as sigma-1 ( $\sigma_1$ ) and sigma-2 ( $\sigma_2$ ) receptor ligands: a review. *Cent. Nerv. Syst. Agents Med. Chem.* **2009**, *9*, 205–219.
- (19) Berardi, F.; Ferorelli, S.; Abate, C.; Colabufo, N. A.; Contino, M.; Perrone, R.; Tortorella, V. 4-(Tetralin-1-yl)- and 4-(naphthalen-1-yl)alkyl derivatives of 1-cyclohexylpiperazine as  $\sigma$  receptor ligands with agonist  $\sigma_2$  activity. *J. Med. Chem.* **2004**, *47*, 2308–2317.
- (20) Abate, C.; Elenewski, J.; Niso, M.; Berardi, F.; Colabufo, N. A.; Azzariti, A.; Perrone, R.; Glennon, R. A. Interaction of the  $\sigma_2$  receptor ligand PB28 with the human nucleosome: computational and experimental probes of interaction with the H2A/H2B dimer. *ChemMedChem.* **2010**, *5*, 268–273.
- (21) Zeng, C.; Vangveravong, S.; Xu, J.; Chang, K. C.; Hotchkiss, R. S.; Wheeler, K. T.; Shen, D.; Zhuang, Z.-P.; Kung, H. F.; Mach, R. H. Subcellular localization of sigma-2 receptors in breast cancer cells using two-photon and confocal microscopy. *Cancer Res.* **2007**, *67*, 6708–6716.
- (22) Zeng, C.; Vangveravong, S.; Jones, L. A.; Hyrc, K.; Chang, K. C.; Xu, J.; Rothfuss, J. M.; Goldberg, M. P.; Hotchkiss, R. S.; Mach, R. H. Characterization and evaluation of two novel fluorescent sigma-2 receptor ligands as proliferation probes. *Mol. Imaging* **2011**, 1–14.
- (23) Azzariti, A.; Colabufo, N. A.; Berardi, F.; Porcelli, L.; Niso, M.; Simone, M. G.; Perrone, R.; Paradiso, A. Cyclohexylpiperazine derivative PB28, a  $\sigma_2$  agonist and  $\sigma_1$  antagonist receptor inhibits cell growth, modulates P-glycoprotein, and synergizes with anthracyclines in breast cancer. *Mol. Cancer Ther.* **2006**, *5*, 1807–1816.
- (24) Ferorelli, S.; Abate, C.; Colabufo, N. A.; Niso, M.; Inglese, C.; Berardi, F.; Perrone, R. Design and evaluation of naphthol- and carbazole-containing fluorescent sigma ligands as potential probes for receptor binding studies. *J. Med. Chem.* **2007**, *50*, 4648–4655.
- (25) Berardi, F.; Colabufo, N. A.; Giudice, G.; Perrone, R.; Tortorella, V.; Govoni, S.; Lucchi, L. New  $\sigma$  and 5-HT<sub>1A</sub> receptor ligands:  $\omega$ -(tetralin-1-yl)-*n*-alkylamine derivatives. *J. Med. Chem.* **1996**, *39*, 176–182.
- (26) Elslager, E. F.; Moore, A. M.; Short, F. W.; Sullivan, J. M.; Tendick, F. H. Synthetic amebicides. II. 7-Dialkylaminoalkylao benz-[*c*]acridines and other 7-aminobenz[*c*]acridines. *J. Am. Chem. Soc.* **1957**, *79*, 4699–4703.
- (27) Perrone, R.; Berardi, F.; Colabufo, N. A.; Leopoldo, M.; Abate, C.; Tortorella, V. *N*-Aryl- or *N*-alkylpiperazine derivatives: the role of *N*-substituent on  $\sigma_1$ ,  $\sigma_2$ , 5-HT<sub>1A</sub>, and D<sub>2</sub> receptor affinity. *Med. Chem. Res.* **2000**, *10*, 201–207.
- (28) Abate, C.; Mosier, P. D.; Berardi, F.; Glennon, R. A. A structure–affinity and comparative molecular field analysis of sigma-2 ( $\sigma_2$ ) receptor ligands. *Cent. Nerv. Syst. Agents Med. Chem.* **2009**, *9*, 246–257.
- (29) Schnitzer, J. E.; Oh, P.; Pinney, E.; Allard, J. Filipin-sensitive caveolae-mediated transport in endothelium: reduced transcytosis, scavenger endocytosis, and capillary permeability of select macromolecules. *J. Cell. Biol.* **1994**, *127*, 1217–1232.
- (30) Gibson, A. E.; Noel, R. J.; Herlihy, J. T.; Ward, W. F. Phenylarsine oxide inhibition of endocytosis: effects on asialofetuin internalization. *Am. J. Physiol.* **1989**, *257*, 182–184.
- (31) Gebreselassie, D.; Bowen, W. D. Sigma-2 receptors are specifically localized to lipid rafts in rat liver membranes. *Eur. J. Pharmacol.* **2004**, *493*, 19–28.
- (32) Torrence-Campbell, C.; Bowen, W. D. Differential solubilization of rat liver sigma-1 and sigma-2 receptors: retention of sigma-2 sites in particulate fractions. *Eur. J. Pharmacol.* **1996**, *304*, 201–210.
- (33) Lajoie, P.; Nabi, I. R. Lipid rafts, caveolae, and their endocytosis. *Int. Rev. Cell. Mol. Biol.* **2010**, *282*, 135–163.
- (34) Patra, S. K. Dissecting lipid raft facilitated cell signaling pathways in cancer. *Biochim. Biophys. Acta* **2008**, *1785*, 182–206.
- (35) Kashiwagi, H.; McDunn, J. E.; Simon, P. O.; Goedegebuure, P. S.; Vangveravong, S.; Chang, K.; Hotchkiss, R. S.; Mach, R. H.; Hawkins, W. G. Sigma-2 receptor ligands potentiate chemotherapies and improve survival in models of pancreatic adenocarcinoma. *J. Transl. Med.* **2009**, *7*, doi:10.1186/1479-5876-7-24.
- (36) Abate, C.; Niso, M.; Contino, M.; Colabufo, N. A.; Ferorelli, S.; Perrone, R.; Berardi, F. 1-Cyclohexyl-4-(4-arylcyclohexyl)piperazines: mixed  $\sigma$  and human  $\Delta_8$ – $\Delta_7$  Sterol Isomerase ligands with antiproliferative and P-Glycoprotein inhibitory activity. *ChemMedChem.* **2011**, *6*, 73–80.
- (37) Wheeler, K. T.; Wang, L. M.; Wallen, C. A.; Childers, S. R.; Cline, J. M.; Keng, P. C.; Mach, R. H. Sigma-2 receptors as a biomarker of proliferation in solid tumours. *Br. J. Cancer* **2000**, *82*, 1223–1232.
- (38) Al-Nabulsi, I.; Mach, R. H.; Wang, L. M.; Wallen, C. A.; Keng, P. C.; Sten, K.; Childers, S. R.; Wheeler, K. T. Effect of ploidy, recruitment, environmental factors, and tamoxifen treatment on the expression of sigma-2 receptors in proliferating and quiescent tumour cells. *Br. J. Cancer* **1999**, *81*, 925–933.
- (39) Hornick, J. R.; Xu, J.; Vangveravong, S.; Tu, Z.; Mitchem, J. B.; Spitzer, D.; Goedegebuure, P.; Mach, R. H.; Hawkins, W. G. The novel sigma-2 receptor ligand SW43 stabilizes pancreas cancer progression in combination with gemcitabine. *Mol. Cancer* **2010**, *9*, 298.
- (40) Hou, C.; Tu, Z.; Mach, R.; Kung, H. F.; Kung, M. P. Characterization of a novel iodinated sigma-2 receptor ligand as a cell proliferation marker. *Nucl. Med. Biol.* **2006**, *33*, 203–209.
- (41) Meech, S. R.; Phillips, D. Photophysics of some common fluorescence standards. *J. Photochem.* **1983**, *23*, 193–217.
- (42) Demas, J. N.; Crosby, G. A. Measurement of photoluminescence quantum yields. A review. *J. Phys. Chem.* **1971**, *75*, 991–1024.
- (43) Matsumoto, R. R.; Bowen, W. D.; Tom, M. A.; Truong, D. D.; De Costa, B. R. Characterization of two novel sigma receptor ligands: antidystonic effects in rats suggest sigma receptor antagonism. *Eur. J. Pharmacol.* **1995**, *280*, 301–310.
- (44) Prism Software, version 3.0 for Windows; GraphPad Software, Inc.: San Diego, CA, 1998.